Chapter 10

RADIATION ISSUES

Contents

10.1 Introduction

All aspects of radiation control at a $\mu^+\mu^-$ collider complex will be folded into the design to insure that compliance with applicable regulations is achieved, and that the accelerators and detectors are operated in a reliable and safe manner. Radiological impact on the work place and on the environment will be kept as low as reasonably achievable (ALARA). This

includes the establishment of a stringent set of radiation limits and design goals for off- and on-site radiation levels, quantification of radiation source terms, specification of shielding design criteria, installation of appropriate radiation instrumentation, provision for access control, and control of residual activation. The entire $\mu^+\mu^-$ collider facility is assumed to be located on the existing Fermilab or BNL sites. This greatly simplifies considerations for monitoring and controlling beam loss induced radiation fields from facility operations. Most of these beam facilities will be within tunneled enclosures (within the dolomite layer) which avoids many potential difficulties.

The basic $\mu^+\mu^-$ collider facility is outlined in [1]. The radiation source terms at this facility are mainly connected with an intense rapid-cycling proton driver, a target station, pion decays in a decay channel, unavoidable muon decays in the accelerator chain and in the final collider and spent muon beam absorption. The first analysis of the radiation environment at muon colliders [2] has shown that the spectrum of radiation issues is wide and challenging. Some of the problems appear to be severe, but can be mitigated with the proposed measures. A series of dedicated simulations have been performed with the MARS code [3] to understand formation of radiation fields in the complex and to assure that there are ways to meet the stringent regulation requirements. Considered in detail are the main collider arcs, the interaction region and absorption of spent muon beam. Although attention is paid mainly to the 2×2 TeV collider, both 2 TeV and 250 GeV muon beams are considered.

The parameters used are from [1]. The radiation levels (per second) around the storage ring are calculated assuming 1000 turns as a beam lifetime and should be multiplied by 10^7 s (collider operational year) when compared to the annual limits. The on-site annual dose limit is taken as 100 mrem/year. The Fermilab off-site limit is 10 mrem/year.

10.2 Proton Source and Muon Production

The proton driver generates $\sim$3 MW of 8 or 30 GeV protons which are directed onto a π-production target. This will require an isolated tunnel with target-vault for π-production, transport line for $\pi \to \mu\nu$ decays and a beam absorber for the spent proton beam. This is similar to the present p-bar production line at Fermilab, except that overall beam power is somewhat higher while the proton energy is lower. A relatively straightforward extension of the p-bar experience should lead to a satisfactory beam handling and shielding solution for the production facility. The entire production region will be well within the existing site and separated from accidental personnel exposure. Isolation and control of the facility would be eased by placing it underground.

10.3 Accelerator Chain

Compared to other parts of the facility, there is nothing serious here, but certainly dedicated studies are required.

10.4 Collider Arc and IR

10.4.1 Source Term

In contrast to hadron colliders, where the interaction points are a serious source of radiation, almost 100% of the prompt radiation in muon collider detectors and in muon storage ring arises in the lattice. The decay length for 2 TeV muons is $\lambda_D \approx 10^7$ m. With 10^{12} muons in a bunch one expects 2×10^5 decays per meter of lattice in a single pass of two bunches. Under the assumed scenario this becomes 2×10^8 decays per meter per store or 6×10^9 decays per meter per second. Electrons from $\mu \to e\nu\overline{\nu}$ decay have a mean energy of approximately 1/3 of that of the muons. These ~ 700 GeV electrons, generated at the rate of 6×10^9 per meter per second, travel to the inside of the ring magnets while radiating many energetic 0.1–1 GeV synchrotron photons towards the outside of the ring [4]. Electromagnetic showers induced by these electrons and photons in the collider components create high radiation levels both in a detector and in the storage ring. Another source of radiation in the muon storage ring is beam halo interactions at limiting apertures, located primarily in the interaction region (IR) optics.

Simulations with the MARS code are done for the realistic lattice described in the previous chapter. All the particle interaction processes are simulated in (1) the lattice with detailed 3-D dipole and quadrupole geometry and magnetic field maps, (2) the 1.45 m radius tunnel surrounded by soil/rock (ρ=2.24 g/cm^3), (3) a 26 m long and 10 m radius experimental hall and (4) the detector are taken into account [4], [5].

A single MARS run includes:

- forced $\mu \to e\nu\overline{\nu}$ decays in the beam pipe (beam muon decay studies) or beam halo interactions with the limiting aperture beam pipe;
- tracking of created electrons in the beam pipe under influence of the magnetic field with emission of synchrotron photons along the track;
- simulation of electromagnetic showers in collider and detector components induced by electrons and synchrotron photons hitting the beam pipe, with production of hadrons and prompt muons via Bethe–Heitler pairs and direct positron annihilation;

- simulation of muon interactions (bremsstrahlung, direct e^+e^- pair production, ionization, deep inelastic nuclear interactions and decays) along the tracks in the lattice, detector, tunnel and experimental hall components and air, and in the surrounding soil/rock;

- simulation of electromagnetic showers initiated at the above muon interaction vertices;

- simulation of hadronic cascades generated in muon and photon interactions, with daughter electromagnetic showers, with muon production (π and K decays, prompt muons in hadronic and electromagnetic interactions), and with low–energy neutron transport;

- histogramming and analysis of particle energy spectra, fluence and energy deposition in various detector and collider regions.

Energy thresholds are 1 MeV for muons and charged hadrons, 0.3 MeV for electrons and photons, and 0.5 eV (0.00215 eV in some cases) for neutrons.

Fig. 10.1 shows particle energy spectra inside the 1.5 cm radius arc aperture for 2 TeV muon decays, while Fig. 10.2 is for particles outside the aperture, averaged over the tungsten liner, magnet components, tunnel air and a few meters of the surrounding soil/rock. In the aperture, one can see a pronounced 700 GeV peak in the decay positron spectrum and a significant number of $\sim$1 GeV photons, whereas most of the particles are rather low energy. Overall mean particle energies and relative multiplicities are given in Table 10.1

Table 10.1: Mean energies of particles and their relative multiplicities in showers induced by 2 TeV μ^+ decays in the arcs averaged over the aperture, magnet components, tunnel air and surrounding soil/rock.

Particle	γ	e^+	e^-	$h^\pm$	n	μ
$\langle$E$\rangle$, MeV	380	12800	63.7	195	0.142	21300
$\langle$N$\rangle$	6120	284	335	0.027	203	0.156

10.4.2 Prompt Radiation

Radiation fields in the lattice components are dominated by electromagnetic showers induced by $\sim$700 GeV decay electrons and positrons and by $\sim$1 GeV synchrotron photons. In the tunnel, experimental hall and in the first meters of the surrounding soil/rock, the field is composed of low energy photons and neutrons. Farther from the tunnel the only significant

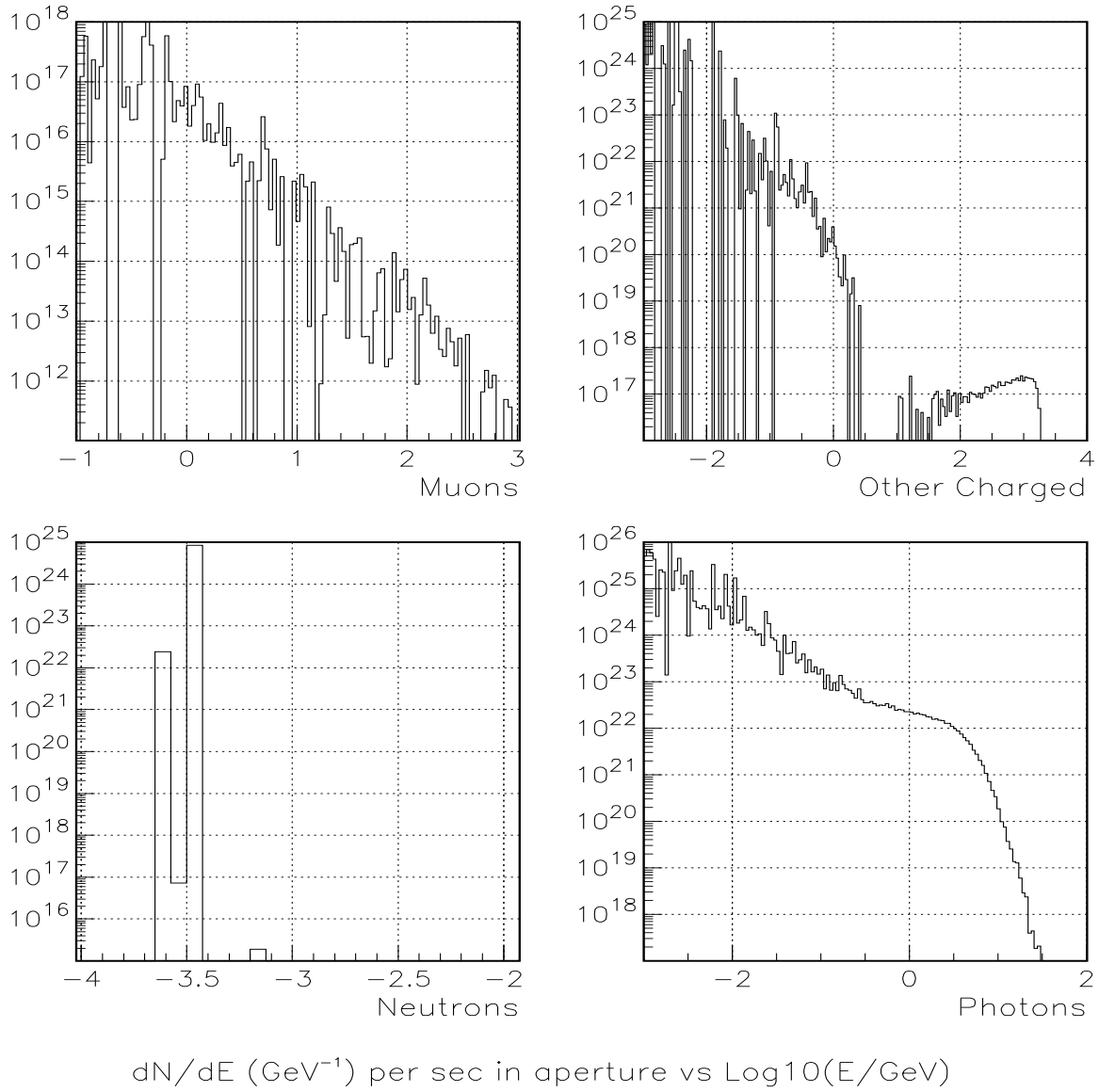

Figure 10.1: Energy spectra of muons, $h^{\pm}$ and $e^{\pm}$, neutrons and photons in the aperture of the arc magnets induced by 2 TeV muon beam decays.

component is muons generated in electromagnetic and hadronic cascades in the magnets. Fig. 10.3 shows isodose contours around the collider tunnel. The distributions are asymmetric in the horizontal plane because of lattice and tunnel curvature and effects of the magnetic field. With 10^7 s as a collider operational year, the tolerable on-site limit in the soil/rock is reached at about 6 m above the orbit plane, 10 m toward the ring center and ~ 75 m outward in the horizontal plane. With 7 m above the ring plane the surface area can even be accessible to the public. All underground facilities (electronics rooms etc.) have to be inside the ring at ≥ 10 m distance from the beam axis. Prompt radiation levels in the experimental hall and

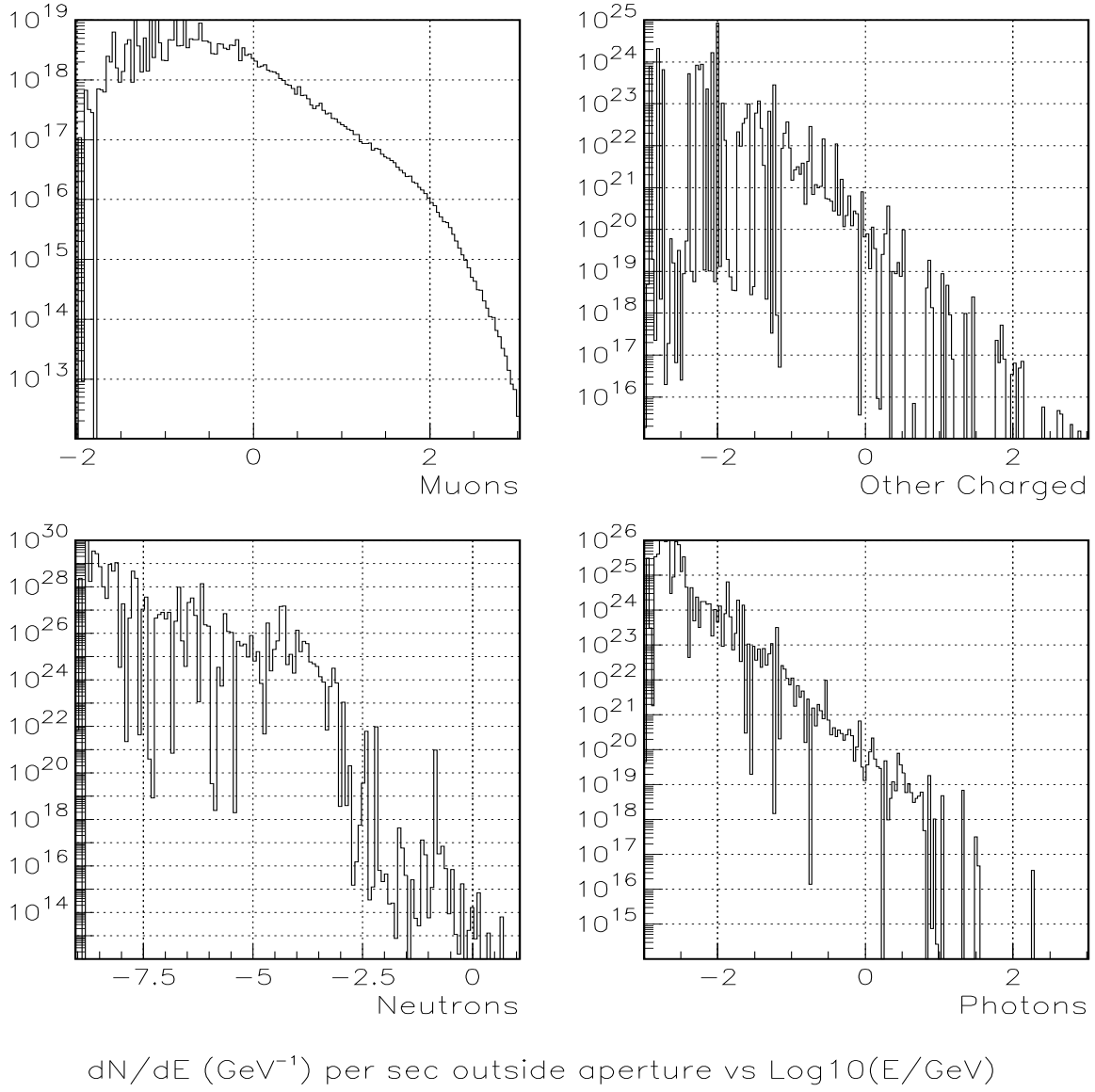

Figure 10.2: Energy spectra of muons, $h^{\pm}$ and $e^{\pm}$, neutrons and photons averaged over the arc magnets, tunnel air and a few meters of the surrounding soil/rock due to 2 TeV muon beam decays.

detector are considered in a separate chapter.

10.4.3 Radioactivation Around Tunnel

In estimating induced radioactivity, the standard approach is based on the number of inelastic nuclear interactions of hadrons with energy ≥ 50 MeV (stars). Star densities in the collider, detector and shielding components can be directly converted into a residual dose rate. Pho-

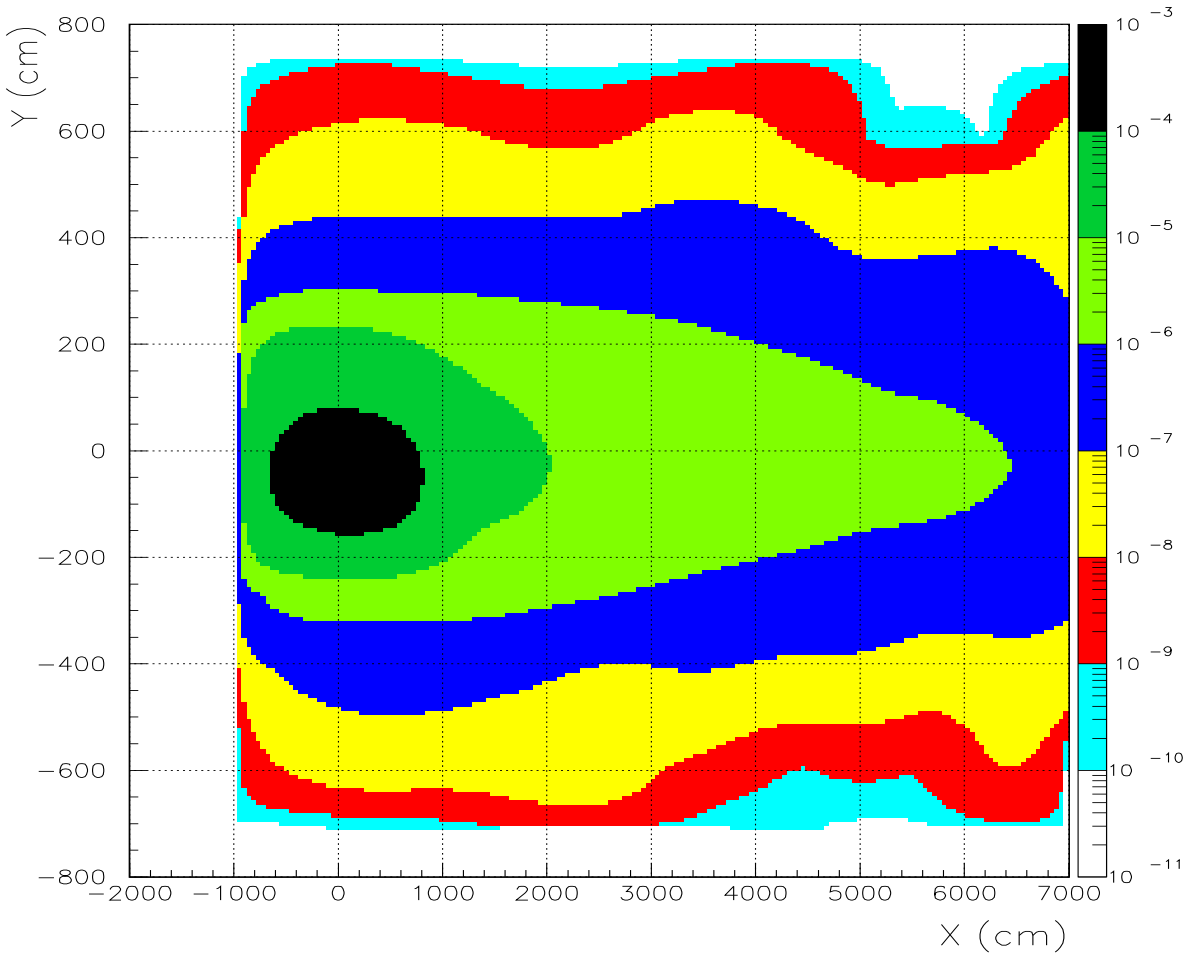

Figure 10.3: Isodose contours in the vertical plane across the collider tunnel and surrounding soil/rock for 2 TeV muon beam decays. y axis is up and x axis points outward along the ring radius. Beam axis is at x=y=0. Right scale is dose rate in rem/sec.

tohadrons in the first layers of the tunnel shielding and hadrons produced along muon tracks farther from the tunnel are a source of soil/rock and groundwater activation around the collider [6]. Two radionuclides, ^{3}H and ^{22}Na, produced in the soil/rock, completely determine the activity concentration that can be found in groundwater. In calculations, isotope production is observed in the first meters around the tunnel, which would require insulation or drainage of that region. The dolomite stratum at Fermilab may naturally satisfy this condition. Further studies are needed.

10.4.4 Radioactivation of Lattice and Detector Components

Due to unavoidable $\mu \to e\nu\overline{\nu}$ decays, about 2 kW of power is deposited in every meter of the collider ring. Generated hadrons induce radioactivation of magnet components. As shown in [2], [5] and in the previous chapter there should be a thick tungsten liner inside the cosine theta magnets to reduce heat load to cryogenics and avoid quench of the superconducting coils. The required thickness of such a liner is 6 cm in the arcs and in the two quadrupoles nearest to the interaction point and about 3 to 4 cm for the most of the interaction region quadrupoles. There is a significant azimuthal dependence of power density and hadron production due to the strong magnetic field. Fig. 10.4 shows the azimuthal distribution of power density in the innermost layer of the tungsten liner in the arc dipoles for a 2 TeV muon beam. The higher peak is due to showers induced by decay positrons (for μ^+ beam) and the

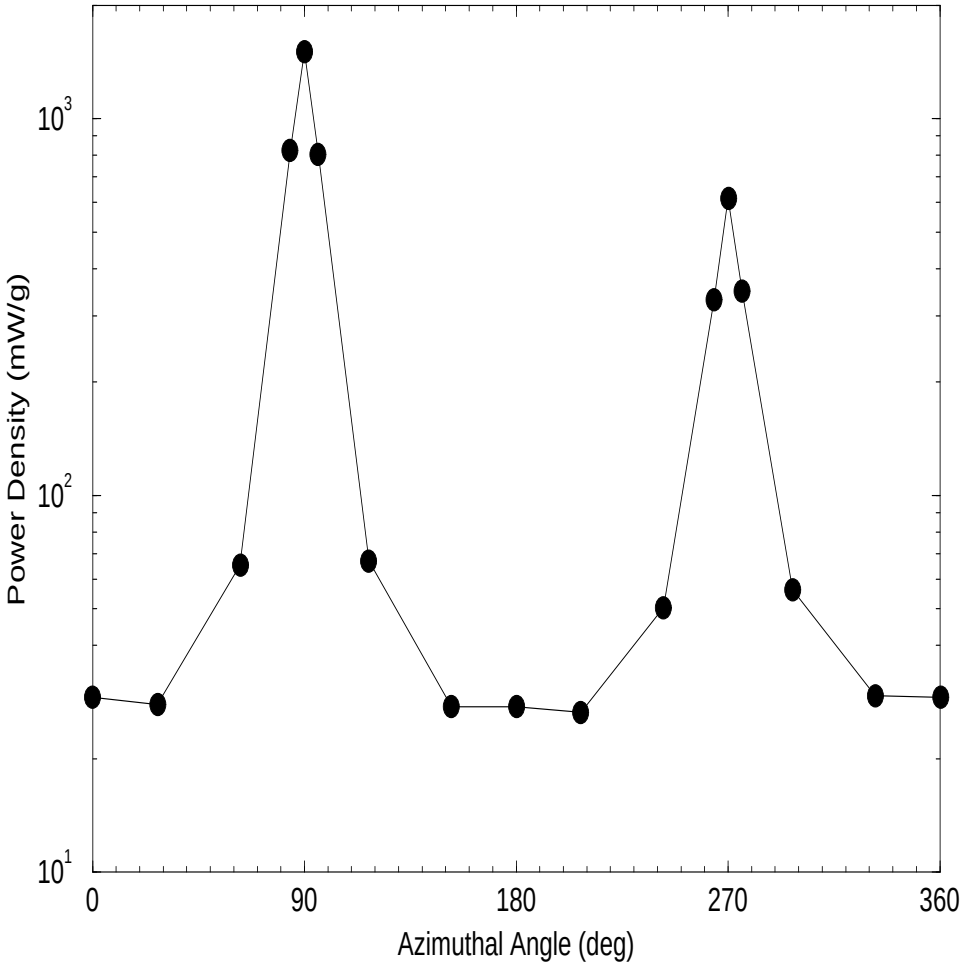

Figure 10.4: Azimuthal distribution of power density in the innermost layer of the tungsten liner inside the arc dipole aperture for 2 TeV muon beam decays.

second peak at the opposite side in the orbit plane is due to synchrotron photons emitted by

positrons. With two beams in the ring, the results presented are simply doubled: electrons hit the inward wall (ϕ=90 deg) and photons hit the outward wall (ϕ=270 deg). Hadron dose and radionuclide production also follow this pattern.

Residual dose rates in magnet components have been estimated assuming a few years of the collider operation and measured immediately after shutdown. With a 6 cm tungsten liner in the arcs, contact dose rate at the inner liner surface is $P_\gamma \sim 9$ rad/hr, at the outer surface $P_\gamma \sim 0.2$ rad/hr, for SC coils and yoke it is $P_\gamma \sim 0.03$ rad/hr, and at the magnet outer shell it is $P_\gamma \sim 0.003$ rad/hr. For the two first quadrupoles in the IR, the tungsten liner is much hotter. The dose rate drops logarithmically with a cooling time (time after shutdown) and at least inversely with the distance from the extended object. For example, the above numbers are 2.3 times smaller 1 day after shutdown.

In the detector region residual dose rate even in the near beam components (tungsten nose) is rather low compared to the machine. Dose rates in the detector drop rapidly with distance from beam axis.

10.5 Spent Beam Absorption

10.5.1 Prompt Radiation

In operating scenarios considered, muons are extracted after about 1000 turns and sent to a beam absorber. Contrary to hadron machines, energy losses extend over a few kilometers (2 TeV case), the absorber needs not be cooled, and spent muon beam can be sent to the soil/rock directly. Fig. 10.5 shows the particle flux attenuation in the soil/rock with a density of ρ=2.24 g/cm^3 for 2 TeV muons. As shown in [6], a characteristic of high-energy muons is the intensive production of electrons, photons and hadrons along the muon vector. The energies of these particles accompanying the muon tracks are sufficient to affect overall flux and dose distributions, and become a source of radionuclide production deep in the rock.

Fig. 10.6 shows isodose contours in the soil/rock for 2 TeV muons. The outer contour coincides with the tolerable on-site dose limit. This is also not very different from the off-site limits. It is 3.55 km long with a maximum width of 18 m at 2.6 km. At small distances, the required radial thickness of soil/rock shielding above the muon beam is 6–7 m which is the same as shielding required for the collider ring. Thus, there is a simple solution to solve the problem: deflect the extracted beam down by 4.5 mrad. With that, muon fluxes are completely confined beneath the ground.

For the 250×250 GeV collider the situation is even easier (see Fig. 10.7): the contour of the allowable on-site dose is only 810 m long with a maximum width of 14.6 m at 700 m.

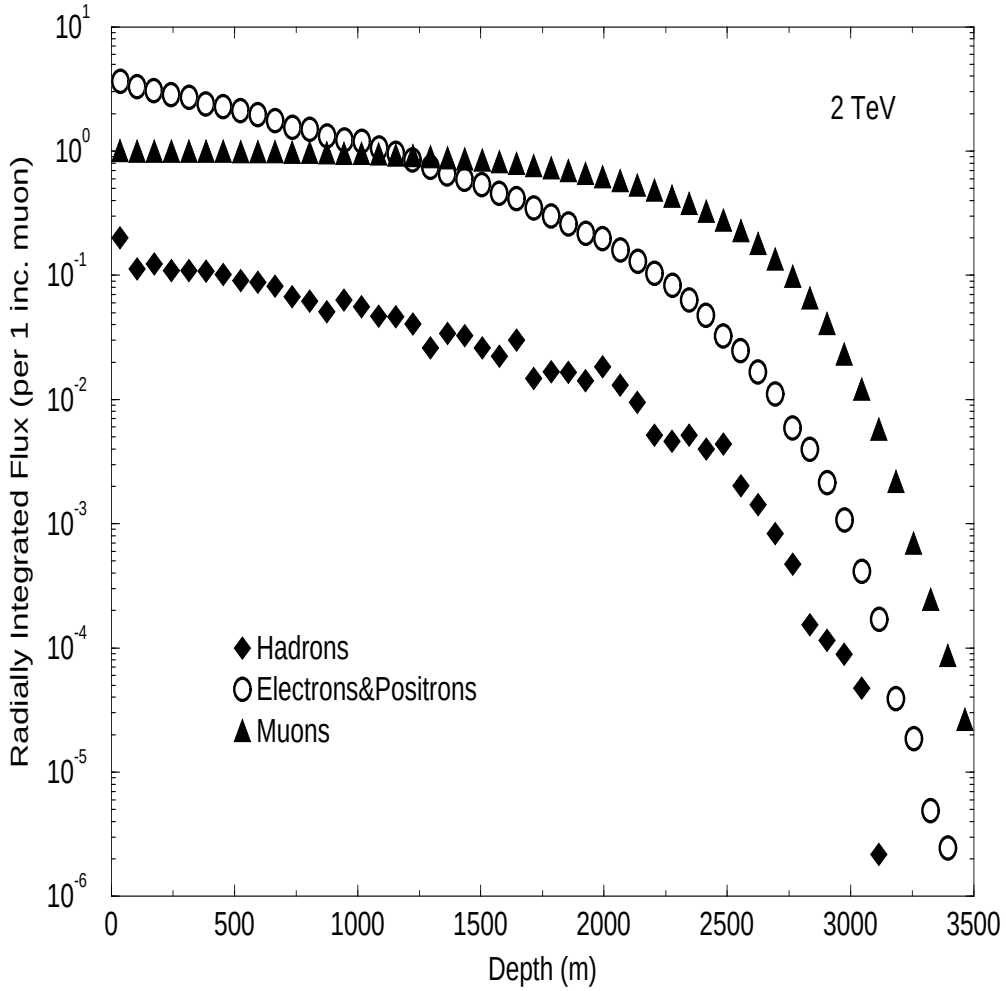

Figure 10.5: Transversely integrated flux of muons, e^+e^- and hadrons in the soil/rock (ρ=2.24 g/cm^3) per one 2 TeV muon beam.

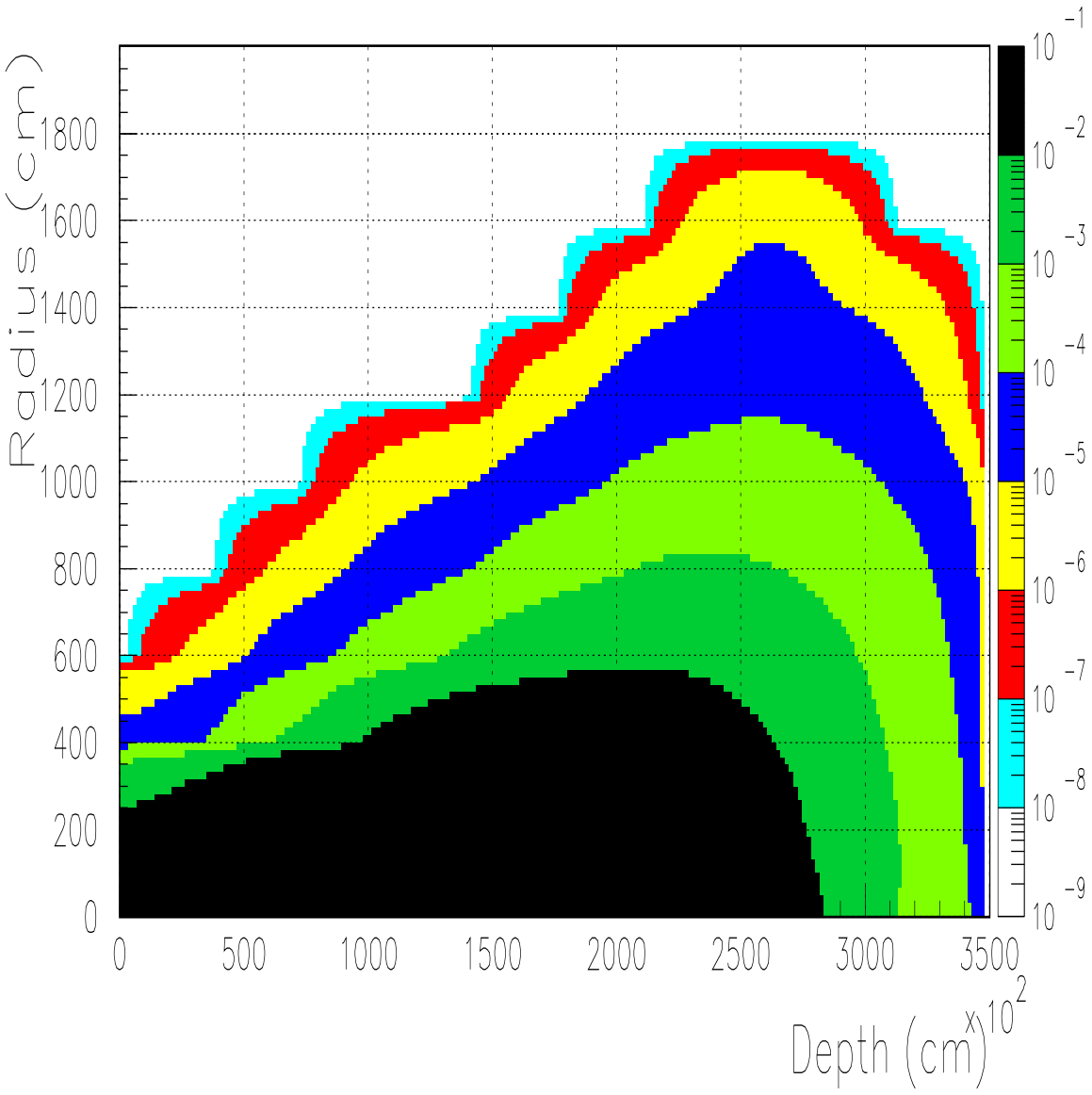

Figure 10.6: Isodose contours in the soil/rock (ρ=2.24 g/cm^3) for 3×10^{13} extracted 2 TeV muons per second. Right scale is dose rate in rem/sec.

Depending on the depth of the ring, $\sim$10 mrad vertical kick down would comply with the regulation requirements.

10.5.2 Radioactivation

As mentioned above, hadrons produced in the interactions along the extracted beam accompany the muon tracks and result in radionuclide production in the soil/rock. Fig. 10.8 and Fig. 10.9 show star density distributions for 2 TeV and 250 GeV muon beams, respectively.

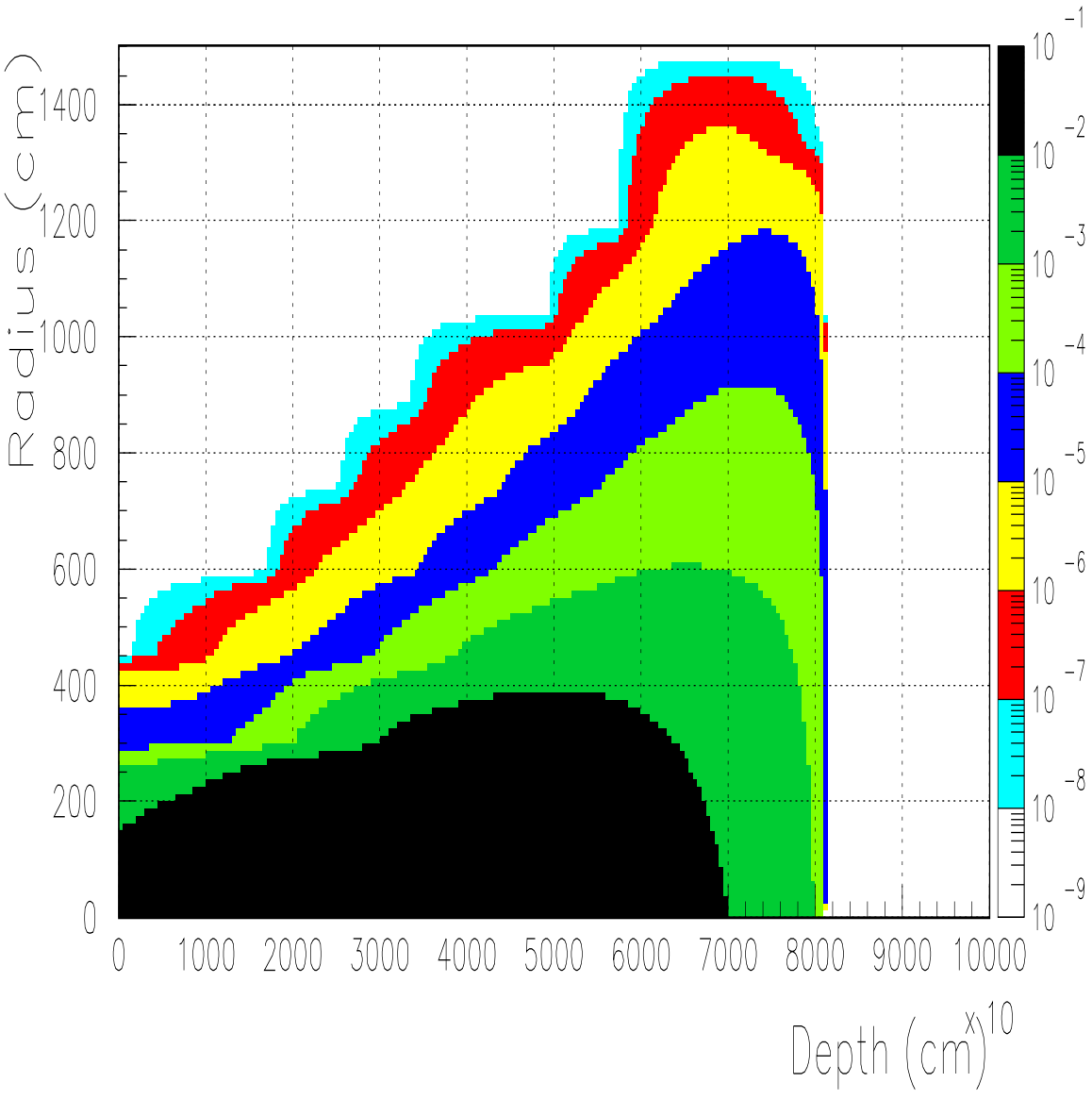

Figure 10.7: Isodose contours in the soil/rock (ρ=2.24 g/cm^3) for 3×10^{13} extracted 250 GeV muons per second. Right scale is dose rate in rem/sec.

Estimates show that at the design parameter operation of a 2×2 TeV collider, the absorp-

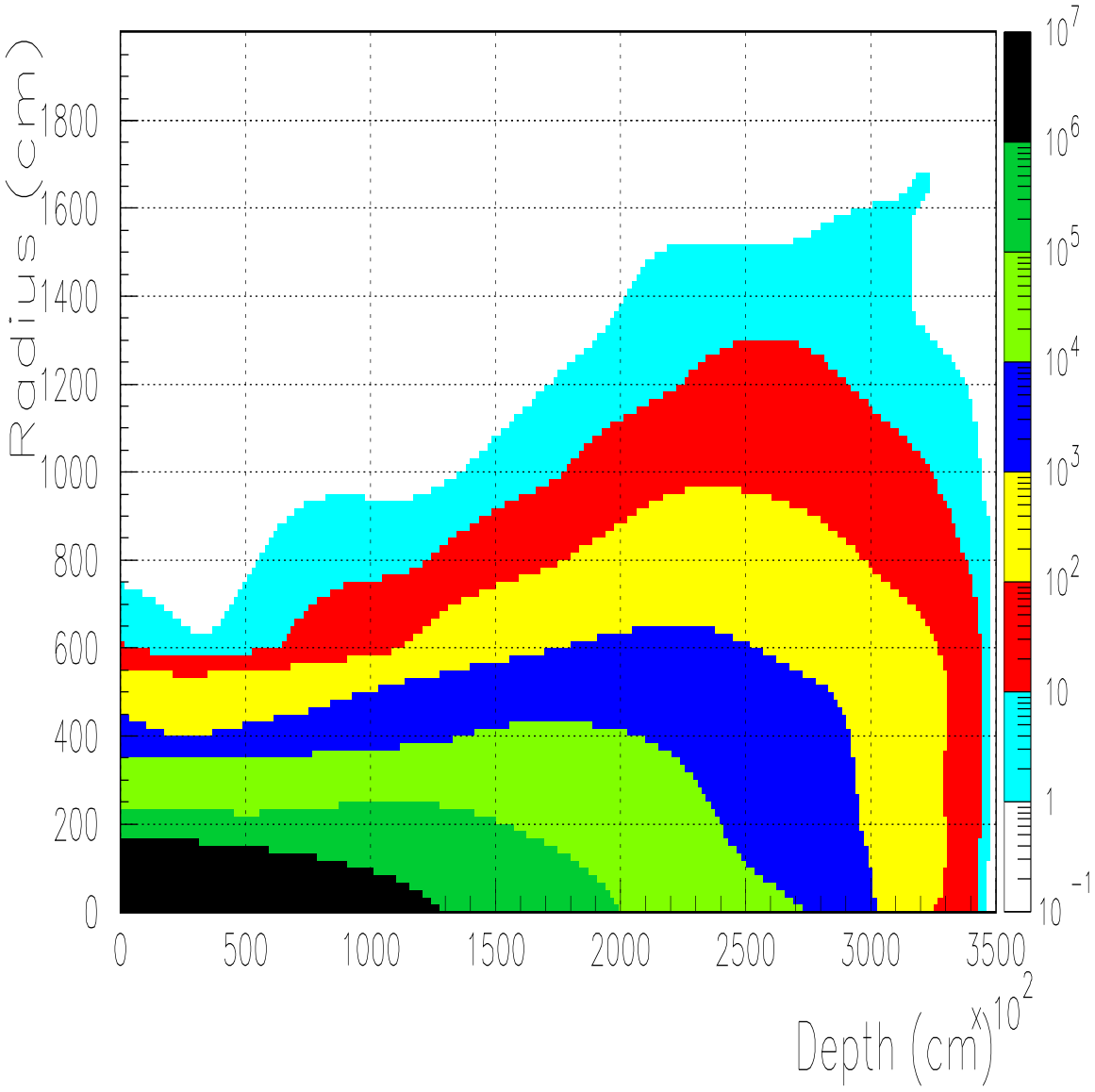

Figure 10.8: Star density contours in the soil/rock (ρ=2.24 g/cm^3) for 3×10^{13} extracted 2 TeV muons per second. Right scale is star density in cm^{-3}s^{-1}.

tion of the spent beam can result in annual activity concentration which may exceed the stringent limits for ^{3}H and ^{22}Na radionuclides, 20 pCi/cm^3 and 0.2 pCi/cm^3 respectively, if the beam disposal lines are in aquiferous layers. The problem is solved if the beam is directed into the impervious dolomite layer (Fermilab) or to an isolated 2.5 km long 2 m radius rock or concrete plug (2 TeV beam). For 250 GeV beam this plug is about 550 m long and 1 m in radius. A steel plug can shorten the indicated dimensions.

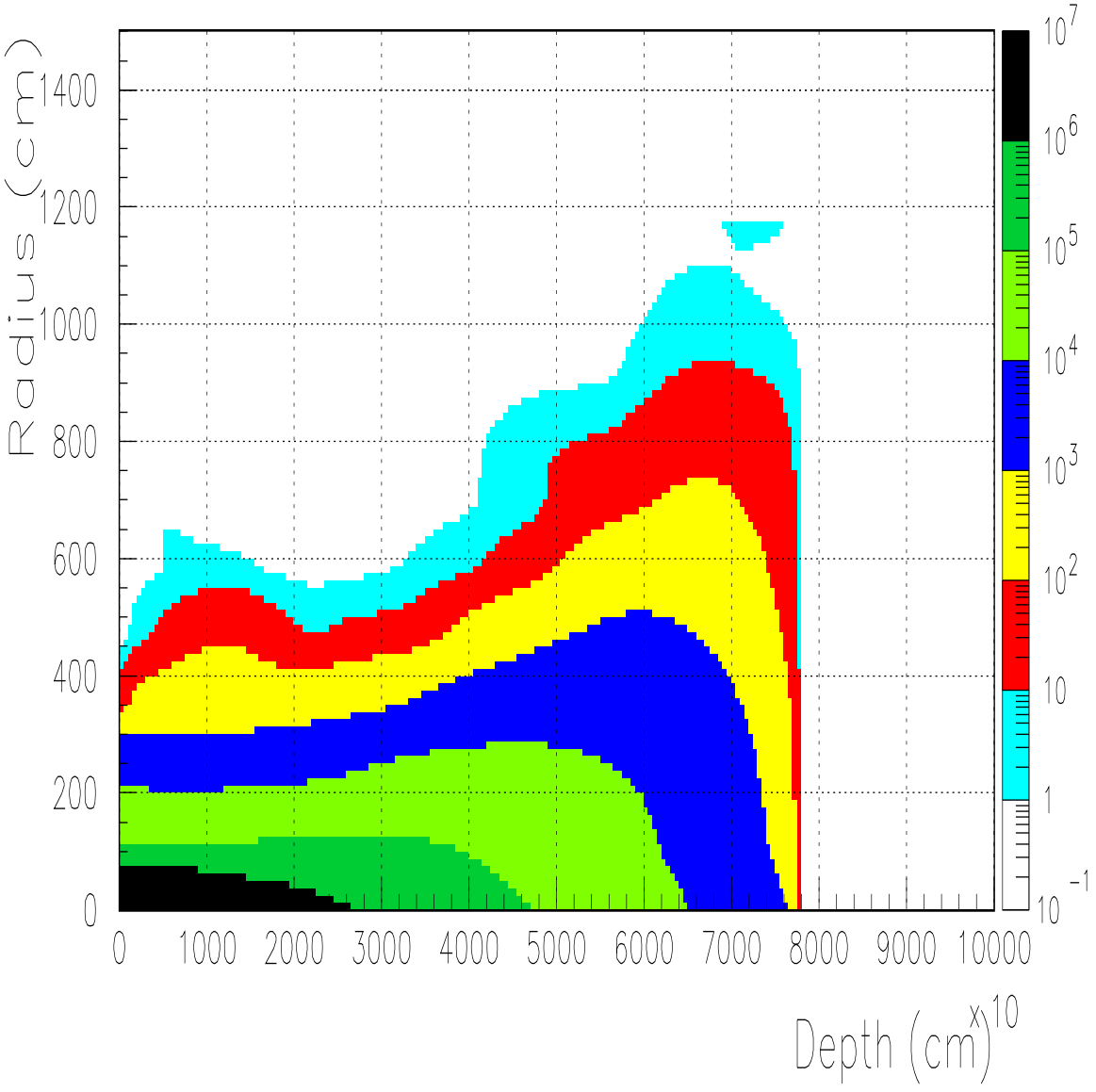

Figure 10.9: Star density contours in the soil/rock (ρ=2.24 g/cm^3) for 3×10^{13} extracted 250 GeV muons per second. Right scale is star density in cm^{-3}s^{-1}.

10.6 Accidental Beam Loss

As at any accelerator facility there is always a non-zero probability for uncontrolled beam loss in a case of a system failure. While the averaged beam power is large, the actual beam energy within the beam pipe in any pulse is relatively small, $\leq 1.4\,\mathrm{MJ}$. This is the largest beam energy that may be lost in a single accident. This is similar to the energy stored in the Tevatron, so similar constraints apply. The big difference is that in all the complex parts except the proton source, the lost particles are the weakly interacting muons, so, contrary to hadron machines, the only concern is a prompt radiation along direction of the lost muon beam. As a first approach the results of the two previous sections are directly applicable to a failure case with a single pulse of $\sim 2 \times 10^{12}$ muons of up to 2 TeV energy. At any location in the facility a single beam accident at 2 TeV and full intensity creates an admissible dose contour in the soil/rock about 2 km long and $\leq 2\,\mathrm{m}$ radius (tangent to the ring if it happens in the collider ring) confined deep beneath the ground within the site boundaries. For the $250 \times 250\,\mathrm{GeV}$ collider, the corresponding contour is much smaller, $\sim 450\,\mathrm{m}$ by $1.5\,\mathrm{m}$.

10.7 Conclusions

In operational mode all radiation problems both for 2 TeV and 250 GeV appear quite solvable. Similarly, no great problems seem to arise from accidental beam loss.

Bibliography

[1] R. Palmer et al., *Muon Collider Design*, BNL–62949, submitted to the Proceedings of the Symposium on Physics Potential and Development of Muon-Muon Colliders, San Francisco, CA, Dec. 1995.

[2] N. V. Mokhov, *The Radiation Environment at Muon Colliders*, in *Proc. of the 2nd Worshop on Simulating Accelerator Radiation Environments (SARE2)*, CERN, October 1995.

[3] N. V. Mokhov, *The* MARS *Code System User's Guide, version 13 (95)*, FNAL–FN–628 (1995).

[4] G. W. Foster and N. V. Mokhov, *Backgrounds and Detector Performance at a 2+2 TeV $\mu^+\mu^-$ Collider*, in *AIP Conference Proceedings*, **352**, pp. 178-190 (1995); also Fermilab–Conf–95/037 (1995).

[5] N. V. Mokhov and S. I. Striganov, *Simulation of Backgrounds in Detectors and Energy Deposition in Superconducting Magnets at $\mu^+\mu^-$ Colliders*, in Proceedings of the 9th Advanced ICFA Beam Dynamics Workshop, Ed. J. C. Gallardo, AIP Conference Proceedings 372, 1996; also Fermilab–Conf–96/011 (1996).

[6] N. V. Mokhov, *Muons at LHC. Part 1: Beam Dumps*, CERN/TIS–RP/TM/95–27 (1995).

Contributors

- N. Mokhov, (FermiLab) Editor

List of Figures

List of Tables